PAPER

Achieving persistent room-temperature phosphorescence from phenanthridone derivatives by molecular engineering†

Hongzhuo Wu,[ab] Deliang Wang,[ac] Jianquan Zhang,[d] Parvej Alam,[d] Zheng Zhao, [ID][d] Yu Xiong, [ID] *[a] Dong Wang[a] and Ben Zhong Tang [ID] *[d]

Organic room-temperature phosphorescence (RTP) materials have emerged as promising candidates for various applications. However, persistent organic RTP materials are still rare and are limited to specific chromophore backbones as most organic molecules possess inefficient intersystem crossing. Herein, a facile molecular engineering strategy is proposed to impart tunable persistent RTP properties to phenanthridone (PTD) derivatives through substituent effects. Notably, by adjusting the electronic effect or position of substituents, an ultralong lifetime of 114.90 ms is achieved in the **PTD-BnCl** crystal. Single-crystal structure analysis shows that the variation in the electronic effect or position of substituents can significantly affect intermolecular interactions and molecular packing, thus giving rise to a remarkable influence on the RTP properties of PTD derivatives in bulk crystals. Furthermore, theoretical calculations not only reveal the mechanism of persistent RTP emission but also elucidate the impact of substituent effects on RTP properties from the molecular and crystalline perspectives, respectively. These simple PTD derivatives with persistent RTP properties are reported for the first time and will help enrich the diversity of organic RTP chromophores.

Introduction

Metal-free organic materials with room-temperature phosphorescence (RTP) properties have attracted widespread attention due to their unique long-lived triplet excitons.[1] In particular, organic RTP materials with an afterglow lasting from seconds to hours show promising application prospects in the fields of optoelectronic devices, with high-sensitivity sensing, high-resolution bioimaging, and advanced anti-counterfeiting properties.[2–5] It is well established that doping rare-earth or noble metal ions into inorganic compounds is an effective way

to obtain an ultralong afterglow that lasts for several hours. However, most rare-earth or noble metals are generally expensive, toxic, and environmentally unfriendly. In 2010, we first proposed the design principle of crystallization-induced phosphorescence, a general crystal engineering approach that can be employed to realize persistent RTP from organic molecules

a Center for AIE Research, Shenzhen Key Laboratory of Polymer Science and Technology, Guangdong Research Center for Interfacial Engineering of Functional Materials, College of Materials Science and Engineering, Shenzhen University, Shenzhen 518061, China. E-mail: xiongyu@szu.edu.cn

b Key Laboratory for Special Functional Materials of Ministry of Education, National & Local Joint Engineering Research Center for High-Efficiency Display and Lighting Technology, Henan University, Kaifeng 475004, China

c Department of Materials Chemistry, Huzhou University, East 2nd Ring Rd. No. 759, Huzhou, 313000, China

d School of Science and Engineering, Shenzhen Institute of Aggregate Science and Technology, The Chinese University of Hong Kong, Shenzhen, Guangdong 518172, China

† Electronic supplementary information (ESI) available. CCDC 2342463–2342468. For ESI and crystallographic data in CIF or other electronic format see DOI: https://doi.org/10.1039/d4tc01387e

Yu Xiong is currently an associate professor at the Shenzhen University (SZU), Shenzhen. She received her PhD degree from the Shanghai Institute of Organic Chemistry, CAS, in 2014. She then worked as a Postdoctoral Fellow under the supervision of Prof. B. S. Ong at the Baptist University from 2015 to 2016 and Prof. B. Z. Tang at the HKUST Shenzhen Research Institute from 2016 to 2019, respectively. She joined the College of Materials Science and Engineering, SZU in 2019. Her research is mainly focused on the development of organic small and polymeric materials with room-temperature phosphorescence and aggregation-induced emission properties.

Yu Xiong

This journal is © The Royal Society of Chemistry 2024

J. Mater. Chem. C, 2024, **12**, 15527–15534 | **15527**

by restricting molecular motions.[6] Since then, metal-free purely organic RTP materials have emerged as ideal alternatives to inorganic afterglow materials due to their advantages of low cost, wide variety, fantastic flexibility, excellent processability, and good biocompatibility. However, the development of organic RTP materials is challenging because most organic molecules have weak spin–orbit coupling (SOC) interactions and very slow radiative decay rates of triplet excitons.[7,8] Therefore, how to improve ISC efficiency and suppress non-radiative decay pathways is a key issue to be resolved in developing efficient and persistent organic RTP materials.

To date, great efforts have been made to achieve persistent organic RTP materials, and significant progress has been achieved. On the one hand, various methods have been proposed to suppress non-radiative relaxation, such as crystal engineering,[6,9] H-aggregation,[10] doping organic phosphors into rigid matrices,[11] deuteration,[12] host–guest complexation,[13] covalent crosslinking,[14] and ionization.[15] On the other hand, strong SOC interactions and a small energy gap between singlet and triplet states (ΔE_{ST}) can improve intersystem crossing (ISC) efficiency. Consequently, molecular design strategies based on the incorporation of heavy atoms (Br and I),[11c,16] carbonyl group,[6,8,17] and heteroatoms (S, N, P, and Se)[15b,18] into organic molecules to enhance SOC interaction have been developed to achieve persistent organic RTP materials. Meanwhile, persistent organic RTP materials can also be obtained by designing organic phosphors with twisted donor–acceptor structures to get small ΔE_{ST} values.[19] For example, we presented a novel design principle to get small ΔE_{ST} values through structural isomerism for the achievement of efficient and ultralong materials.[20] Notably, organic RTP can be activated by the presence of a trace amount of impurity.[21] Despite these great achievements, persistent organic RTP materials are still rare and limited to specific organic chromophore skeletons such as carbazole, benzophenone, phenothiazine, diphenyl sulfoxide/sulphone, and so on.[1,22] Therefore, developing a facile and effective design strategy based on molecular engineering to enrich the diversity of organic chromophores with persistent RTP properties is of significant importance and urgent need.

It is well known that intermolecular interactions and molecular packing also play crucial roles in tailoring the luminescence behaviors of macroscopic aggregates in addition to the intrinsic electronic structures.[23] Accordingly, typical design principles such as devising new chromophores, alkyl sidechain engineering, and substituent effects have been reported to achieve the desired RTP properties. Herein, owing to the convenient structural modification and the inclusion of a carbonyl group to promote the ISC process, the planar and electron-deficient phenanthridone (PTD) framework with a fused π-conjugated aromatic lactam structure is selected as a promising candidate for the construction of organic RTP emitters. As far as we know, using the PTD skeleton as the building block for constructing organic RTP materials has not been reported yet.[24] Consequently, by simply introducing different substituents (Br, Cl, and CN) into the benzyl unit and PTD skeleton, respectively, a series of PTD derivatives, namely **PTD-BnBr**, **PTD-BnCl**, **PTD-**
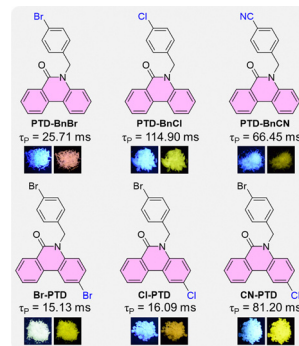

Fig. 1 The chemical structures of PTD derivatives **PTD-BnBr**, **PTD-BnCl**, **PTD-BnCN**, **Br-PTD**, **Cl-PTD**, and **CN-PTD**, and their RTP properties in crystalline states, respectively.

BnCN, **Br-PTD**, **Cl-PTD**, and **CN-PTD** are designed and synthesized for the development of organic RTP materials (Fig. 1). Notably, the structure–property relationship can be established by studying the impact of substituent effects on the RTP properties. As expected, all PTD derivatives exhibited persistent RTP properties with lifetimes on the scale of milliseconds. Particularly, RTP properties can be regulated effectively by changing the electronic effect or position of substituents. On the one hand, an ultralong lifetime of 114.90 ms was obtained by introducing a halogen Cl atom into the benzyl unit; on the other hand, the introduction of a strong electron-withdrawing CN group into the PTD skeleton is more conducive to improving RTP properties. The results of single-crystal structure analysis and theoretical calculations indicate that the persistent RTP properties of these PTD derivatives are determined by their intrinsic excited-state electronic structures, intermolecular interactions, and molecular packing in bulk crystals. Besides, the promising applications of these PTD derivatives in the fields of anti-counterfeiting and information encryption were demonstrated by employing a time-gated approach to modulate the organic afterglow duration.

Results and discussion

The PTD derivatives **PTD-BnBr**, **PTD-BnCl**, **PTD-BnCN**, **Br-PTD**, **Cl-PTD**, and **CN-PTD** were readily synthesized by a nucleophilic substitution reaction between the corresponding PTD and benzyl bromide in medium to high yields (Scheme S1, ESI†), and carefully characterized by ^{1}H NMR, ^{13}C NMR, high-resolution mass spectroscopy, single-crystal X-ray diffraction, and elemental analyses.

The photophysical properties of PTD derivatives were first studied in dilute THF solutions. As illustrated in Fig. 2a, the PTD derivatives **PTD-BnBr**, **PTD-BnCl**, and **PTD-BnCN** with substituents located on the benzyl unit display similar absorption spectra with three sets of absorption bands in the range of 200–350 nm. In contrast, the absorption spectra of PTD derivatives **Br-PTD**, **Cl-PTD**, and **CN-PTD** with substituents located on the PTD core are different, among which the absorption profile of **CN-PTD** is significantly blue-shifted relative to the other two (Fig. 2b). Accordingly, the PTD derivatives **PTD-BnBr**, **PTD-BnCl**, and **PTD-**
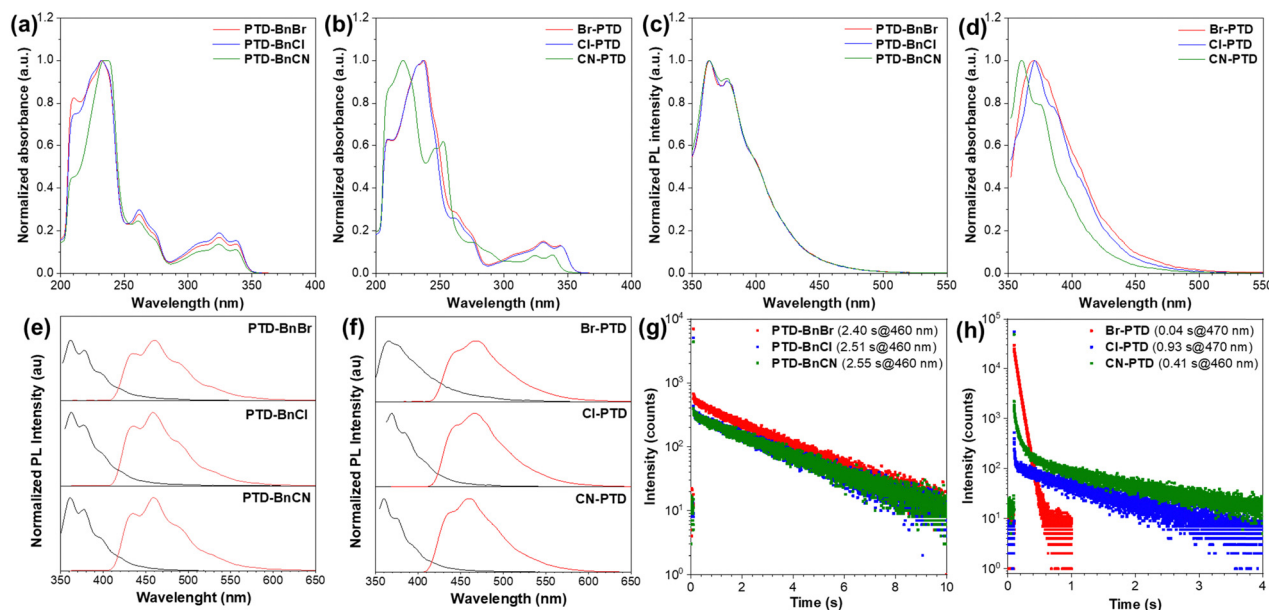
Fig. 2 Photophysical properties of PTD derivatives **PTD-BnBr**, **PTD-BnCl**, **PTD-BnCN**, **Br-PTD**, **Cl-PTD**, and **CN-PTD** in dilute THF solutions (10^{-5} M): (a) and (b) UV-vis absorption and (c) and (d) steady-state PL spectra at room temperature; (e) and (f) prompt and delayed PL spectra (delay 1 ms) at 77 K; (g) and (h) time-resolved phosphorescence decay curves at 77 K. The excitation wavelength for delayed PL spectra and corresponding decay curves is set to be 340 nm.

BnCN exhibit similar fluorescence emission bands featuring a fine structure originating from the radiative transition of local excited states, while the fluorescence emission band of **CN-PTD** undergoes a remarkable blue-shift (Fig. 2c and d). These results indicate that the electronic structures of PTD derivatives hardly change when different substituents are introduced into the benzyl unit, while the introduction of different substituents on the PTD core causes significant changes. Additionally, the theoretical calculations of frontier molecular orbitals performed on PTD derivatives in the gas phase show that both the HOMO and LUMO are locally distributed on the PTD core, which can well explain the impact of substituent effects on the absorption and fluorescence emission behaviors (Fig. S1, ESI†). More importantly, these PTD derivatives dissolved into dilute solutions exhibit a persistent

afterglow at a low temperature of 77 K (Fig. S2, ESI†). As shown in Fig. 2e, the three PTD derivatives **PTD-BnBr**, **PTD-BnCl**, and **PTD-BnCN** exhibit very similar low-temperature phosphorescence spectra with maximum emission peaks located at ∼460 nm. By fitting delayed emission decay curves, the ultralong lifetimes of **PTD-BnBr**, **PTD-BnCl**, and **PTD-BnCN** are estimated to be 2.40, 2.51, and 2.55 s respectively, indicating that molecular motions are effectively restricted at cryogenic temperature (Fig. 2g). However, the RTP lifetimes of PTD derivatives **Br-PTD**, **Cl-PTD**, and **CN-PTD** are very different despite their similar phosphorescence emission profiles, which indicates that the substituents have a significant influence on the excited triplet states. In a word, the substituents on the PTD core have a more significant impact on the photophysical properties at the molecular level (Table 1).

Considering that these PTD derivatives show excellent low-temperature phosphorescence in dilute solutions, their luminescence properties in crystals were investigated under ambient conditions. As illustrated in Fig. 3a and b, a remarkable redshift between the prompt and delayed PL spectra was observed, indicating that all PTD derivatives displayed dual-emission of fluorescence and RTP in the crystal. Additionally, by fitting the prompt and delayed PL decay curves of these PTD derivatives, the prompt fluorescence and RTP emission lifetimes were estimated to be on the scale of nanoseconds and milliseconds, respectively (Fig. 3c and d and Fig. S3, ESI†), further confirming their persistent RTP properties in crystals. Compared with the PL spectra in dilute solutions, the remarkable redshift of PL spectra in crystals should be due to intermolecular interactions upon aggregation. Interestingly, despite their similar photophysical properties in dilute solutions, PTD derivatives **PTD-BnBr**, **PTD-BnCl**, and **PTD-BnCN** exhibit different RTP properties in crystals (Table S1, ESI†), among which an ultralong lifetime of

Table 1 Summary of photophysical parameters of PTD derivatives **PTD-BnBr**, **PTD-BnCl**, **PTD-BnCN**, **Br-PTD**, **Cl-PTD**, and **CN-PTD** in dilute solutions and crystals, respectively

	Solutions			Crystals				
Compounds	λ_F (nm)	$\lambda_{P\text{-}77\,K}$ (nm)	$\tau_{P\text{-}77\,K}$ (s)	λ_F (nm)	τ_F (ns)	λ_P (nm)	τ_P (ms)	Φ_{PL} (%)
PTD-BnBr	362	460	2.40	390	1.33	571	25.71	10.3
PTD-BnCl	362	461	2.51	387	0.91	546	114.90	5.5
PTD-BnCN	361	459	2.55	381	0.26	546	66.45	5.4
Br-PTD	365	468	0.04	399	0.40	567	15.13	0.9
Cl-PTD	369	466	0.93	401	0.83	558	16.09	2.7
CN-PTD	360	460	0.41	401	0.45	556	81.20	3.2

λ_F: fluorescent emission; $\lambda_{P\text{-}77\,K}$: phosphorescent emission at 77 K; $\tau_{P\text{-}77\,K}$: phosphorescent lifetime at 77 K; λ_P: phosphorescent emission; τ_F: fluorescent lifetime; τ_P: phosphorescent lifetime; Φ_{PL}: total photoluminescence quantum yield.

This journal is © The Royal Society of Chemistry 2024

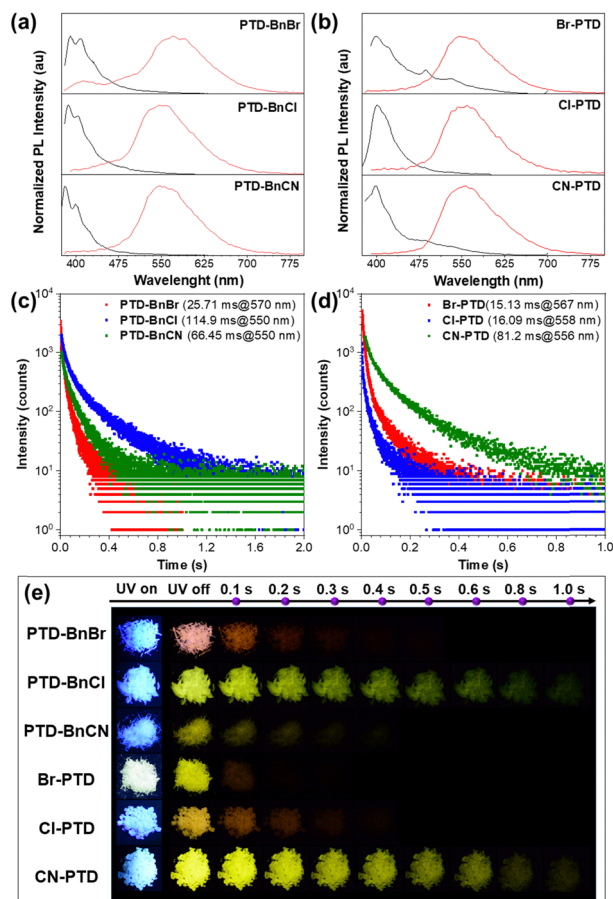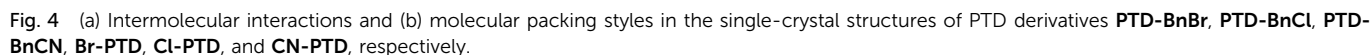*J. Mater. Chem. C*, 2024, **12**, 15527–15534 | **15529**

Fig. 3 The photophysical properties of PTD derivatives **PTD-BnBr**, **PTD-BnCl**, **PTD-BnCN**, **Br-PTD**, **Cl-PTD**, and **CN-PTD** in crystals at room temperature: (a) and (b) prompt and delayed PL spectra (delay 1 ms); (c) and (d) time-resolved phosphorescence decay curves; (e) luminescence photographs under and after removing the UV irradiation (365 nm). The excitation wavelength for delayed PL spectra and corresponding decay curves is set to be 360 nm, except **Br-PTD** and **Cl-PTD** which is 330 nm.

114.90 ms can be obtained when a Cl atom is introduced as a substituent on the benzyl unit. Although the other three PTD derivatives **Br-PTD**, **Cl-PTD**, and **CN-PTD** also exhibited different RTP properties in crystals, the longest lifetime was achieved for the cyano-substituted PTD derivative **CN-PTD**. Notably, their PL quantum yields are reduced compared with PTD derivatives containing substituents on the benzyl unit, which indicates that the introduction of substituents onto the PTD core may lead to more severe fluorescence quenching. Compared to most organic RTP molecules reported in the literature, the quantum yields are not high enough (Scheme S1, ESI†). Besides, all PTD derivatives show an obvious yellowish-green afterglow to the naked eye (Fig. 3e). These experimental results demonstrate that changes in the substituent position or type have a profound impact on the RTP properties of these PTD derivatives at the aggregate level.

Given that crystals of these PTD derivatives show distinct luminescence properties from dilute solutions, single-crystal structure analysis was performed to understand the effects of intermolecular interactions and molecular packing on their crystalline luminescence properties. As depicted in Fig. 4a, all

these PTD derivatives show similar twisted molecular geometries, but different torsion angles of 89.16°, 77.88°, 87.61°, 73.8°, 72.97°, and 82.37° are presented in **PTD-BnBr**, **PTD-BnCl**, **PTD-BnCN**, **Br-PTD**, **Cl-PTD**, and **CN-PTD** respectively. These extremely distorted molecular conformations are beneficial to prevent the formation of overtight molecular packing to avoid aggregation-caused quenching. Furthermore, a variety of intermolecular interactions are formed in the crystal structures of these PTD derivatives (Table 2). A single **PTD-BnBr** molecule participates in only a few weak C–H···π intermolecular interactions. In contrast, abundant intermolecular interactions including multiple C–H···O=C, C–H···π, C–H···N≡C, and O=C···π are formed in individual **PTD-BnCl** and **PTD-BnCN** molecules. Under these different intermolecular interactions, the PTD derivatives **PTD-BnBr**, **PTD-BnCl**, and **PTD-BnCN** form different molecular packings. As shown in Fig. 4b, **PTD-BnCl** and **PTD-BnCN** exhibit a herringbone stacking pattern, while **PTD-BnCl** adopts a compact packing mode with a 2D extended framework structure. By contrast, the nonradiative decay in the **PTD-BnCl** crystal is better suppressed, and persistent RTP with an ultralong lifetime of 114.90 ms is finally obtained. On the other hand, abundant intermolecular interactions exist in PTD derivatives **Br-PTD**, **Cl-PTD**, and **CN-PTD**, among which each **CN-PTD** molecule can form up to twelve intermolecular interactions with neighboring molecules. More importantly, tight π···π stacking is formed in the halogen-substituted PTD derivatives **Br-PTD** and **Cl-PTD**, while slipped face-to-face stacking without π···π interaction is formed in the cyano-substituted PTD derivative **CN-PTD**. Generally, most organic chromophores with planar π-conjugation structure tend to form tight π···π stacking which leads to the well-known aggregation-caused quenching effect.[25] Consequently, the RTP properties of **Br-PTD** and **Cl-PTD** is poor compared to that of **CN-PTD** due to the π–π stacking interaction. The single-crystal structure analysis demonstrates that the RTP properties in crystals are mainly determined by the synergistic effects of highly distorted geometry, multiple intermolecular interactions, and ordered molecular packing.

The first-principles density functional theory (DFT) and time-dependent DFT calculations were performed on PTD derivatives in the crystal phase to reveal the mechanism of persistent RTP emission. As illustrated in Fig. 5, the three PTD derivatives **PTD-BnBr**, **PTD-BnCl**, and **PTD-BnCN** show similar energy level diagrams, in which five triplet states are located below S_1, thus five possible ISC processes can readily occur between S_1 and the low-lying triplet states ($S_1 \rightarrow T_n$, $n = 1$–5). The SOC constants $\xi(S_1$–$T_n)$ and $\xi(S_0$–$T_1)$ calculated to be **PTD-BnBr**, **PTD-BnCl**, and **PTD-BnCN** are relatively considerable, which can ensure an effective population of triplet excitons and subsequent radiative transition of T_1. In contrast, the three PTD derivatives **Br-PTD**, **Cl-PTD**, and **CN-PTD** show bigger differences in energy level diagrams and SOC constants. For **Br-PTD** and **Cl-PTD**, five triplet states lie below S_1, thus five possible ISC processes can occur between S_1 and the low-lying triplet states ($S_1 \rightarrow T_n$, $n = 1$–5). Owing to the heavy-atom effect, **Br-PTD** has larger SOC constants $\xi(S_1$–$T_n)$ and $\xi(S_0$–$T_1)$, resulting in the

Fig. 4 (a) Intermolecular interactions and (b) molecular packing styles in the single-crystal structures of PTD derivatives **PTD-BnBr**, **PTD-BnCl**, **PTD-BnCN**, **Br-PTD**, **Cl-PTD**, and **CN-PTD**, respectively.

more efficient production of triplet excitons. For **CN-PTD**, six possible ISC processes can occur between S_1 and the low-lying triplet states ($S_1 \rightarrow T_n$, $n = 1$–6). The small ΔE_{ST} of 0.07 eV between S_1 and T_6 can also promote ISC, thus leading to the efficient generation of triplet excitons. Meanwhile, the slipped face-to-face stacking without $\pi \cdots \pi$ interaction formed in the **CN-PTD** crystal also contributes to preventing the quenching of triplet excitons. Therefore, **CN-PTD** crystal shows the best RTP properties. Besides, we calculated the natural transition orbitals (NTOs) of S_1 and T_1 to provide a qualitative description of the electronic configuration (Fig. S4, ESI†). According to El-Sayed's rules,[26] the ISC is favored if the transition between S and T states involves a change of molecular orbital ($^1\pi\pi^*$ to $^3n\pi^*$ and $^1n\pi^*$ to $^3\pi\pi^*$). Hybrid transitions consisting of $\pi\pi^*$ and $n\pi^*$ transitions are observed for all PTD molecules. The composition of hybrid transitions changes slightly as different substituents are introduced into the benzyl unit, while the proportion of $n\pi^*$ transitions increases significantly when halogen atoms are introduced onto the PTD core (Table S1, ESI†). This qualitative description is consistent with the corresponding calculated SOC constants $\xi(S_0–T_1)$. These calculations suggest that the persistent RTP properties of these PTD derivatives in bulk crystals should be attributed to the intrinsic excited-state electronic structures as well as intermolecular interactions and molecular packing.

Finally, the potential applications of these PTD derivatives with different afterglow durations in the fields of anti-counterfeiting and information encryption are demonstrated

This journal is © The Royal Society of Chemistry 2024

J. Mater. Chem. C, 2024, **12**, 15527–15534 | **15531**

Table 2 Summary of intermolecular interactions in the single-crystal structures of PTD derivatives **PTD-BnBr**, **PTD-BnCl**, **PTD-BnCN**, **Br-PTD**, **Cl-PTD**, and **CN-PTD**

PTD-derivatives	Intermolecular interactions
PTD-BnBr	C–H···π: 2.866, 2.888 Å
PTD-BnCl	C–H···O=C: 2.545, 2.531 Å
	C–H···π: 2.869, 2.812 Å
PTD-BnCN	C–H···N≡C: 2.576, 2.639 Å
	C–H···O=C: 2.580
	O=C···π: 3.037, 3.172 Å
	C–H···π: 2.856, 2.855 Å
Br-PTD	C–H···O=C: 2.509 Å
	C–H···H–C: 2.278 Å
	C–H···Br: 2.987 Å; C–H···π: 2.797 Å
	π···π: 3.375 Å Br···Br: 3.612 Å
Cl-PTD	C–H···H–C: 2.255 Å
	C–H···O=C: 2.506 Å
	C–H···π: 2.755 Å
	π···π: 3.399 Å
CN-PTD	C–H···O=C: 2.665 Å
	C–H···N≡C: 2.483
	Br···π: 3.536, 3.456 Å
	C–H···π: 2.842, 2.884 Å

Fig. 6 Potential applications of PTD derivatives in the fields of advanced anti-counterfeiting and information encryption.

through a time-gated method. As shown in Fig. 6, the term "PTD" consists of three encoding materials with different afterglow colors and lifetimes. Under the irradiation of 365 nm UV light, the word " PTD" shows a colorful fluorescence. After ceasing the UV irradiation, the colored fluorescence of the word "PTD" turns into afterglow with different colors. As time goes by, the letters "P" and "T" with shorter afterglow duration disappear successively, while the letter "D" is still visible to the naked eye until 1 second.

Conclusions

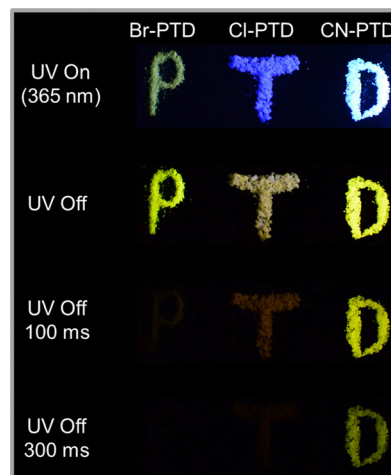In summary, a series of simple PTD derivatives containing Br, Cl or CN groups on the benzyl unit or PTD skeleton were easily synthesized *via* nucleophilic substitution reactions. In dilute solutions, these PTD derivatives exhibit dual-emission through prompt fluorescence and ultralong low-temperature phosphorescence. It is worth noting that similar ultralong lifetimes of 2.40, 2.51, and 2.55 s are estimated for **PTD-BnBr**, **PTD-BnCl**, and **PTD-BnCN** respectively. In comparison, there is a huge difference in the low-temperature phosphorescence lifetime of **Br-PTD**, **Cl-PTD**, and **CN-PTD**, which is 0.04, 0.93, and 0.40 s respectively. This indicates that the introduction of substituents on the PTD core has a more significant impact on the photophysical properties at the molecular level. From solutions to bulk crystals, the phosphorescence lifetimes of PTD derivatives are remarkably reduced. However, an ultralong RTP lifetime is obtained for the PTD derivative containing a Cl group on the benzyl group (114.90 ms for **PTD-BnCl**) or a CN group on the PTD core (81.20 ms for **CN-PTD**), respectively. More importantly,
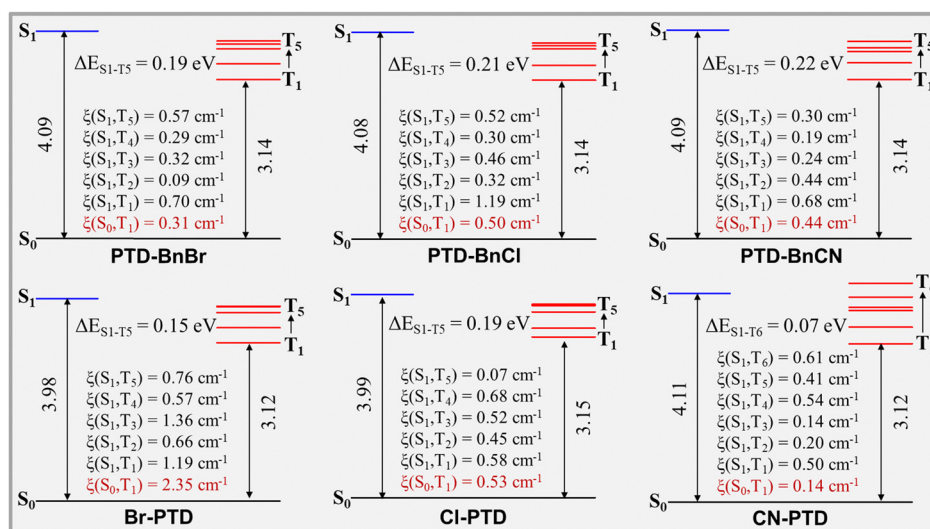

Fig. 5 Calculated energy level diagrams, spin−orbit coupling (SOC) constants between the involved S_n and T_n states of PTD derivatives **PTD-BnBr**, **PTD-BnCl**, **PTD-BnCN**, **Br-PTD**, **Cl-PTD**, and **CN-PTD**, respectively.

15532 | *J. Mater. Chem. C*, 2024, **12**, 15527–15534

This journal is © The Royal Society of Chemistry 2024

single-crystal structure analysis and theoretical calculations show that the RTP lifetime of PTD derivatives containing substituents on the benzyl unit is mainly determined by intermolecular interactions and molecular packing in the crystal, given their similar intrinsic low-temperature phosphorescence properties. In the meantime, the intrinsic electronic structure, intermolecular interactions, and molecular packing play an important role in regulating the RTP properties of PTD derivatives by modifying the PTD core with various substituents. To the best of our knowledge, tunable persistent RTP behavior is achieved for the first time in these simple PTD derivatives by modulating either the electronic effects or positions of substituents and demonstrates the importance of substituent effects for tunable photophysical properties in molecular aggregates. We believe that this work will provide important guidance for the exploration of novel organic RTP materials.

Author contributions

H. Z. Wu carried out most of the experiments. D. L. Wang performed the theoretical calculations. J. Q. Zhang and P. Alam helped in data collection. Z. Zhao assisted in data analysis. Y. Xiong performed data analysis and wrote the manuscript. D. Wang and B. Z. Tang revised the manuscript.

Data availability

The data supporting this article have been included as part of the ESI.†

Conflicts of interest

There are no conflicts to declare.

Acknowledgements

Notes and references

1 (a) J. Yang, M. Fang and Z. Li, *InfoMat*, 2020, **2**, 791–806; (b) W. Zhao, Z. He and B. Z. Tang, *Nat. Rev. Mater.*, 2020, **5**, 869–885; (c) J. Guo, C. Yang and Y. Zhao, *Acc. Chem. Res.*, 2022, **55**, 1160–1170; (d) S. Cai, X. Yao, H. Ma, H. Shi and Z. An, *Aggregate*, 2023, **4**, e320; (e) S. Cai, X. Yao, H. Ma, H. Shi and Z. An, *Aggregate*, 2023, **4**, e320; (f) Q. Zhou,

C. Yang and Y. Zhao, *Chem*, 2023, **9**, 2446; (g) B. Ding, X. Ma and H. Tian, *Acc. Mater. Res.*, 2023, **4**(10), 827–838.

2 (a) R. Kabe, N. Notsuka, K. Yoshida and C. Adachi, *Adv. Mater.*, 2016, **28**, 655–660; (b) T. Wang, X. Su, X. Zhang, X. Nie, L. Huang, X. Zhang, X. Sun, Y. Luo and G. Zhang, *Adv. Mater.*, 2019, **31**, 1904273; (c) C. F. Si, T. Wang, A. K. Gupta, D. B. Cordes, A. M. Z. Slawin, J. S. Siegel and E. Zysman-Colman, *Angew. Chem., Int. Ed.*, 2023, **62**, e202309718; (d) X. Wu, X. Peng, L. Chen, B. Z. Tang and Z. Zhao, *ACS Mater. Lett.*, 2023, **5**, 664–672.

3 (a) A. Fermi, G. Bergamini, M. Roy, M. Gingras and P. Ceroni, *J. Am. Chem. Soc.*, 2014, **136**, 6395–6400; (b) Y. Zhou, W. Qin, C. Du, H. Gao, F. Zhu and G. Liang, *Angew. Chem., Int. Ed.*, 2019, **58**, 12102–12106; (c) P. Ashokkumar, N. Adarsh and A. S. Klymchenko, *Small*, 2020, **16**, 2002494; (d) Q. Zhou, Y. X. Liu, X. R. Ma, W. W. Fan, Y. Cheng, R. Y. He, X. Meng, Y. G. Shi, Q. E. Cao, L. Y. Zheng and L. Wang,, *Adv. Opt. Mater*, 2024, DOI: **10.1002/adom.202303107**.

4 (a) G. Zhang, G. M. Palmer, M. W. Dewhirst and C. L. Fraser, *Nat. Mater.*, 2009, **8**, 747; (b) X. Zhen, Y. Tao, Z. An, P. Chen, C. Xu, R. Chen, W. Huang and K. Pu, *Adv. Mater.*, 2017, **29**, 1606665; (c) Y. F. Zhang, J. S. Li, J. L. Zhao, X. F. Li, Z. M. Wang, Y. C. Huang, H. K. Zhang, Q. Liu, Y. X. Lei and D. Ding, *Angew. Chem., Int. Ed.*, 2024, **63**, e202313890; (d) K. Chang, L. Xiao, Y. Fan, J. Gu, Y. Wang, J. Yang, M. Chen, Y. Zhang, Q. Li and Z. Li, *Sci. Adv.*, 2023, **9**, eadf6757.

5 (a) Y. Su, S. Z. F. Phua, Y. Li, X. Zhou, D. Jana, G. Liu, W. Q. Lim, W. K. Ong, C. Yang and Y. Zhao, *Sci. Adv.*, 2018, **4**, eaas9732; (b) D. Wang, J. Gong, Y. Xiong, H. Wu, Z. Zhao, D. Wang and B. Z. Tang, *Adv. Funct. Mater.*, 2022, **33**, 2208895; (c) X. Zhang, J. You, J. Zhang, C. Yin, Y. Wang, R. Li and J. Zhang, *CCS Chem.*, 2023, **5**, 2140–2215; (d) H. Deng, G. Li, H. Xie, Z. Yang, Z. Mao, J. Zhao, Z. Yang, Y. Zhang and Z. Chi, *Angew. Chem., Int. Ed.*, 2024, **63**, e202317631.

6 W. Yuan, X. Shen, H. Zhao Jacky, W. Y. Lam, L. Tang, P. Lu, C. Wang, Y. Liu, Z. Wang, Q. Zheng, J. Sun, Y. Ma and B. Tang, *J. Phys. Chem. C*, 2010, **114**, 6090–6099.

7 M. A. El-Sayed, *Acc. Chem. Res.*, 1968, **1**, 8–16.

8 W. Zhao, Z. He Jacky, W. Y. Lam, Q. Peng, H. Ma, Z. Shuai, G. Bai, J. Hao and B. Z. Tang, *Chem*, 2016, **1**, 592–602.

9 O. Bolton, K. Lee, H. J. Kim, K. Y. Lin and J. Kim, *Nat. Chem.*, 2011, **3**, 205.

10 Z. An, C. Zheng, Y. Tao, R. Chen, H. Shi, T. Chen, Z. Wang, H. Li, R. Deng, X. Liu and W. Huang, *Nat. Mater.*, 2015, **14**, 685–690.

11 (a) M. S. Kwon, D. Lee, S. Seo, J. Jung and J. Kim, *Angew. Chem., Int. Ed.*, 2014, **53**, 11177; (b) D. Lee, O. Bolton, B. C. Kim, J. H. Youk, S. Takayama and J. Kim, *J. Am. Chem. Soc.*, 2013, **135**, 6325; (c) Z. A. Yan, X. Lin, S. Sun, X. Ma and H. Tian, *Angew. Chem., Int. Ed.*, 2021, **60**, 19735; (d) H. Wu, D. Wang, Z. Zhao, D. Wang, Y. Xiong and B. Z. Tang, *Adv. Funct. Mater.*, 2021, **31**, 2101656; (e) J.-A. Li, L. Zhang, C. Wu, Z. Huang, S. Li, H. Zhang, Q. Yang, Z. Mao, S. Luo, C. Liu, G. Shi and B. Xu,

This journal is © The Royal Society of Chemistry 2024

J. Mater. Chem. C, 2024, **12**, 15527–15534 | **15533**

Angew. Chem., Int. Ed., 2023, **62**, e202217284; (*f*) Y. S. Zhou, P. Zhang, Z. Liu, W. Q. Yan, H. Y. Gao, G. D. Liang and W. Qin, *Adv. Mater.*, 2024, DOI: **10.1002/adma.202312439**.

12 S. Hirata, K. Totani, H. Kaji, M. Vacha, T. Watanabe and C. Adachi, *Adv. Opt. Mater.*, 2013, **1**, 438–442.

13 Z. Y. Zhang, W. W. Xu, W. S. Xu, J. Niu, X. H. Sun and Y. Liu, *Angew. Chem., Int. Ed.*, 2020, **59**, 18748–18754.

14 (*a*) F. F. Shen, Y. Chen, X. Y. Dai, H. Zhang, B. Zhang, Y. H. Liu and Y. Liu, *Chem. Sci.*, 2021, **12**, 1851–1857; (*b*) J. A. Li, C. Wu, Z. Huang, S. Li, H. Zhang, Q. Yang, Z. Mao, S. Luo, C. Liu, G. Shi and B. Xu, *Angew. Chem., Int. Ed.*, 2023, **62**, e202217284..

15 (*a*) H. Wang, H. Shi, W. Ye, X. Yao, Q. Wang, C. Dong, W. Jia, H. Ma, S. Cai, K. Huang, L. Fu, Y. Zhang, J. Zhi, L. Gu, Y. Zhao, Z. An and W. Huang, *Angew. Chem., Int. Ed.*, 2019, **58**, 18776–18782; (*b*) P. Alam, T. S. Cheung, N. L. C. Leung, J. Zhang, J. Guo, L. Du, R. T. K. Kwok, J. W. Y. Lam, Z. Zeng, D. L. Phillips, H. H. Y. Sung, I. D. Williams and B. Z. Tang, *J. Am. Chem. Soc.*, 2022, **144**, 3050–3062; (*c*) J. Wang, X. Gu, H. Ma, Q. Peng, X. Huang, X. Zheng, S. H. P. Sung, G. Shan, J. W. Y. Lam, Z. Shuai and B. Z. Tang, *Nat. Commun.*, 2018, **9**, 2963.

16 (*a*) S. Sarkar, H. P. Hendrickson, D. Lee, F. DeVine, J. Jung, E. Geva, J. Kim and B. D. Dunietz, *J. Phys. Chem. C*, 2017, **121**, 3771–3777; (*b*) T. Zhu, T. Yang, Q. Zhang and W. Z. Yuan, *Nat. Commun.*, 2022, **13**, 2658; (*c*) Y. He, J. Wang, Q. Li, S. Qu, C. Zhou, C. Yin, H. Ma, H. Shi, Z. Meng and Z. An, *Adv. Opt. Mater.*, 2023, **11**, 2201641.

17 (*a*) S. Zheng, T. Zhu, Y. Wang, T. Yang and W. Z. Yuan, *Angew. Chem., Int. Ed.*, 2020, **59**, 10018–10022; (*b*) H. Chen, Y. Sun, M. Liu, F. Li, Q. Peng and H. Huang, *Angew. Chem., Int. Ed.*, 2023, **135**, e202302629.

18 Z. Wang, X. Cheng, Y. Xie, S. Liu, M. Dong, J. Zhao, F. Liang, Z. An and W. Huang, *CCS Chem.*, 2023, **5**, 292–309.

19 (*a*) H. Uoyama, K. Goushi, K. Shizu, H. Nomura and C. Adachi, *Nature*, 2012, **492**, 234–238; (*b*) Z. Yang, Z. Mao, Z. Xie, Y. Zhang, S. Liu, J. Zhao, J. Xu, Z. Chi and M. P. Aldred, *Chem. Soc. Rev.*, 2017, **46**, 915–1016.

20 Y. Xiong, Z. Zhao, W. Zhao, H. Ma, Q. Peng, Z. He, X. Zhang, Y. Chen, X. He, J. W. Y. Lam and B. Z. Tang, *Angew. Chem., Int. Ed.*, 2018, **57**, 7997–8001.

21 (*a*) C. Chen, Z. Chi, K. C. Chong, A. S. Batsanov, Z. Yang, Z. Mao, Z. Yang and B. Liu, *Nat. Mater.*, 2020, **20**, 175–180; (*b*) B. B. Ding, L. W. Ma, Z. Z. Huang, X. Ma and H. Tian, *Sci. Adv.*, 2021, **7**, eabf9668; (*c*) Z. Wu, J. C. Roldao, F. Rauch, A. Friedrich, M. Ferger, F. Wurthner, J. Gierschner and T. B. Marder, *Angew. Chem., Int. Ed.*, 2022, **61**, e202200599; (*d*) A. Mazarevics, K. Leduskrasts and E. Suna, *ACS Mater. Lett.*, 2024, **6**, 2703–2713.

22 (*a*) A. D. Nidhankar, Goudappagouda, V. C. Wakchaure and S. S. Babu, *Chem. Sci.*, 2021, **12**, 4216–4236; (*b*) S. Guo, W. Dai, X. Chen, Y. Lei, J. Shi, B. Tong, Z. Cai and Y. Dong, *ACS Mater. Lett.*, 2021, **3**, 379–397; (*c*) W. Shao and J. Kim, *Acc. Chem. Res.*, 2022, **55**, 1573–1585; (*d*) X. Yang, G. I. N. Waterhouse, S. Y. Lu and J. H. Yu, *Chem. Soc. Rev.*, 2023, **52**, 8005–8058.

23 (*a*) Y. Shoji, Y. Ikabata, Q. Wang, D. Nemoto, A. Sakamoto, N. Tanaka, J. Seino, H. Nakai and T. Fukushima, *J. Am. Chem. Soc.*, 2017, **139**, 2728–2733; (*b*) E. Lucenti, A. Forni, C. Botta, L. Carlucci, C. Giannini, D. Marinotto, A. Pavanello, A. Previtali, S. Righetto and E. Cariati, *Angew. Chem., Int. Ed.*, 2017, **56**, 16302–16307; (*c*) J. Wang, Z. Chai, J. Wang, C. Wang, M. Han, Q. Liao, A. Huang, P. Lin, C. Li, Q. Li and Z. Li, *Angew. Chem., Int. Ed.*, 2019, **58**, 17297–17302; (*d*) Q. Li and Z. Li, *Acc. Chem. Res.*, 2020, **53**, 962–973; (*e*) W. Liu, J. Wang, Y. Gong, Q. Liao, Q. Dang, Z. Li and Z. Bo, *Angew. Chem., Int. Ed.*, 2020, **59**, 20161–20166; (*f*) E. Hamzehpoor and D. F. Perepichka, *Angew. Chem., Int. Ed.*, 2020, **59**, 9977–9981; (*g*) M. X. Gao, J. Ren, Y. X. Gong, M. M. Fang, J. Yang and Z. Li, *Aggregate*, 2023, DOI: **10.1002/agt2.462**.

24 (*a*) D. Attila and B. Tibor, *J. Phys. Chem. A*, 2001, **105**, 4611–4621; (*b*) X. H. Duan, C. H. Pei and Y. J. Ma, *Sci. China, Ser. B: Chem.*, 2008, **51**, 632–639.

25 Q. Li and Z. Li, *Adv. Sci.*, 2017, **4**, 1600484.

26 M. A. El-Sayed, *Acc. Chem. Res.*, 1968, **1**, 8.

15534 | *J. Mater. Chem. C*, 2024, **12**, 15527–15534

This journal is © The Royal Society of Chemistry 2024